Full-Fledged 10Base-T Ethernet Underwater Optical Wireless Communication System

Giulio Cossu, Alessandro Sturniolo, Alessandro Messa, David Scaradozzi, and Ernesto Ciaramella, *Senior Member, IEEE*

***Abstract*— Marine researchers and operators during their daily work need consistent data from the underwater environment to constantly monitor the habitat's probes and the robots condition. For underwater applications, wireless communication is of paramount importance. Today, the needs for high-speed communication has prompted the exploration of the Underwater Optical Wireless Communications (UOWCs) method. This paper presents the design and validation aspects of the optical layer of a bidirectional UOWC system developed in the framework of the European Project SUNRISE, able to provide wireless connectivity compliant to 10Base-T Ethernet protocol (Manchester-coded signal with 10 Mb/s data rate). The designed modems are made of two similar optical transceivers, each including a transmitter, a receiver unit, and an optical power monitor part. The transmitter is based on an array of blue Light Emitting Diodes; the receiver exploits a commercially available Avalanche Photodiode (APD) and the monitoring relies on a pin-photodiode. The modems, after a deep characterization in controlled environments, were proved to work with the required 10Base-T Ethernet, up to 7.5 m distance in shallow harbor waters. The complete optical system is intended to become a node of the SUNRISE infrastructure.**

***Index Terms*— Underwater communication, visible light communication, light emitting diodes, wireless communication.**

I. Introduction

THE rising number of human underwater activities increases the need for efficient systems and devices deputed at sea-monitoring, ranging from buoys, ships, Underwater Sensor Networks (UWSNs), Remotely Operated Vehicles (ROVs) and Autonomous Underwater Vehicles (AUVs) [1]. Unmanned underwater vehicles are today a mature technology, which is stimulating also the research towards multi-vehicles coordinated operation [2]–[5]. A key tasks of these vehicles is to record and transmit data to a central unit, e.g. staff on a ship, in particular high-resolution images, and videos. Transferring this type of data timely requires high bit-rate transmission. Vehicles are sometimes forced to use wired solutions, which have limited applications, since they impact on device mobility and re-configurability [5].

Manuscript received February 22, 2017; revised July 15, 2017; accepted September 16, 2017. Date of publication November 16, 2017; date of current version January 5, 2018. This work was supported by the European Union through the ICT FP7 Project "SUNRISE" under Grant 611449 (subproject). *(Corresponding author: Giulio Cossu.)*

G. Cossu, A. Sturniolo, A. Messa, and E. Ciaramella are with Scuola Superiore Sant'Anna University, 56124 Pisa, Italy (e-mail: g.cossu@santannapisa.it).

D. Scaradozzi is with the Dipartimento di Ingegneria dell'Informazione, Università Politecnica delle Marche, 60131 Ancona, Italy.

Color versions of one or more of the figures in this paper are available online at http://ieeexplore.ieee.org.

Digital Object Identifier 10.1109/JSAC.2017.2774702

Due to the strong attenuation of radiofrequencies (RFs) in water [6]–[9], today the applications requiring vehicle mobility mostly rely on acoustic modems [10]. Although low-frequency waves can travel over long distances [11], high-frequency acoustic waves suffer from strong absorption and mechanical limitations, which make them unsuitable. Therefore the available bandwidth of common acoustic modems is around few kHz which strongly limits the maximum bit-rate [12]: high-end acoustic modems can have a transmission rate up to 35 kbit/s [13]. Furthermore underwater acoustic transmission is strongly affected by noise, generated by different sources.

In order to provide for both high-speed and wireless operation, Underwater Optical Wireless Communications (UOWC) is an attractive alternative, which is rapidly gaining momentum. Particularly, UOWC is also synergically driven by achievements in the area of terrestrial (indoor) Visible Light Communications, which have recently shown various practical solutions and very high bit rates, using low-cost Light Emitting Diodes (LEDs) [14]–[18].

UOWC usually exploits the visible region where the sea-water presents a low-attenuation window. Compared to acoustic modems, UOWC can offer much higher bit-rates although on shorter distances: depending on bit rate and water attenuation, this technology can reach Mbit/s rates over distances of tens of meters [19]–[22].

UOWC systems were proposed based on Laser Diodes (LDs) or LEDs. LDs have wider bandwidth and higher optical power but suffer from misalignment, and are more expensive compared to LEDs. First UOWC results were taken using LDs [23], [24]. Recently LEDs were also considered in [25]. All these remarkable results, however suffer from the several strong limitations that can have a key role when considering practical implementations: the channel has almost ideal transmission with very low attenuation, the transmission distance is short ($<$10 m), there is no relevant external noise sources (e.g., sunlight). Mostly, in the papers cited above, UOWC systems were working on dry setups, being both the transmitter (TX) and the receiver (RX) outside the water, hence with no the need for waterproof packaging. Furthermore the channel was the clean and still water of an indoor pool, thus having no turbidity, no relevant turbulence and controlled background illumination.

Recently, we used blue LEDs to demonstrate 58 Mb/s in 2.5 m clear water channel transmission with Discrete Multitone, in an outdoor pool with a waterproof TX and RX, both submerged [26]. The system was working with strong

sunlight illumination, which poses a severe limitation to the achievable Optical Signal to Noise Ratio (OSNR).

In the framework of the EU-FP7 SUNRISE project [27], we designed and realized a complete bidirectional UOWC system that could be integrated in the project's network of underwater things, complementing the capability of acoustic modems. The system is made of two modems, each including the photonic layer, the Ethernet layer and its related software. They are inserted in an underwater case and are designed to provide a reliable 10Base-T IEEE standard bi-directional transmission (10 Mbit/s Ethernet) over at least 10 m in shallow harbor waters (high turbidity and high loss) and daylight condition [28], [29]. Each modem can be an additional node integrated in the test-bed of the SUNRISE infrastructure. The integration is not limited to the physical connection, but also extends to the user control by means of the SUNSET framework [27].

Here we report on the design and experimental assessment of the optical layer of that novel UOWC system; the system is based on an array of LEDs as transmitter and a commercially available avalanche photodiode (APD) as receiver. The modem has been first designed and then deeply characterized both in lab and underwater, in terms of background light and channel attenuation. The setup has been tested in a real underwater scenario with the two modems immersed in the outdoor sea of the La Spezia harbor. To the best of our knowledge, this research is the first attempt to realize a pair of bidirectional optical modems that are field-tested in a harsh underwater environment (high turbidity) and resilient to a strong ambient light (Italy Summer days). Moreover, our modems are completely compliant with the Ethernet standard data transmission. No Digital Signal Processing (DSP) is required, thus reducing the overall cost and the latency of the modems.

This paper is organized as follows. In section II, we describe the key limiting effects in our UOWC case. In section III, we present the optical layer design of the proposed modem and the equipment used for the demonstration. In section IV, we report the results obtained in the lab to characterize the optical components and the system performance. In section V, we report the underwater case design of the proposed modem used for the demonstration. In section VI, we show the results of the preliminary sea-trials measurements performed at La Spezia harbor, namely at NATO's Centre for Maritime Research and Experimentation (CMRE) and at the Italian Navy's Centro di Supporto e Sperimentazione Navale (CSSN) facilities.

II. Underwater Optical Wireless Communication

Electromagnetic (EM) waves are a faster communication media compared to acoustic waves are strongly attenuated in water mainly due to absorption and scattering. Fig. 1 shows the EM attenuation spectrum in a wide spectral range [30]. As example, an attenuation coefficient k of 10 m^{-1} introduces an attenuation of 43 dB after 1 m transmission. It can be clearly seen that in the visible region there is a minimum of attenuation, around the blue wavelength. The exact wavelength of the minimum depends on the characteristics of the

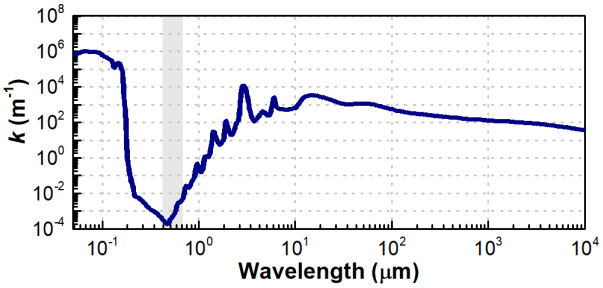

Fig. 1. Typical attenuation coefficient in water in a wide spectral range.

specific water. As example, for clear water, this minimum is at 470 nm. The wavelength increases for murkier water [31].

The effects of scattering and absorption can be modeled with a mathematical equation combined with the common propagation formula of the free-space channel at zero frequency (DC). A LED radiation pattern can be approximated as a Lambertian emission [32], hence the free-space propagation at distance d between transmitter and receiver is given by [33]

$$H(0) = \frac{m+1}{2\pi d^2} \cos^{\mathrm{m}}(\phi)\, A_{RX}\, f(\psi)\, g(\psi) \cos(\psi) \qquad (1)$$

where ϕ is the radiation angle, ψ is the incident angle at the receiver, A_{RX} is the active area of the photo-detector, f and g represent the transmittance of the optical filter and the optical gain of the lens at the receiver, respectively. In (1) we can see the proportionality to d^{-2}, typical of free-space links.

As said, the two most relevant phenomena in UOWC are absorption and scattering, which result in the loss of intensity or change in direction of an optical wave, respectively. The absorption is due to both inorganic and organic substances [13]. Scattering, resulting in the deflection of the light from the original direction, also leads to the intensity reduction of the signal. The overall underwater losses are thus usually expressed by the attenuation coefficient $k(\lambda)$:

$$k(\lambda) = a(\lambda) + b(\lambda), \qquad (2)$$

where $a(\lambda)$ and $b(\lambda)$ coefficients are the absorption and the scattering coefficients, respectively.

We can neglect the impulse response of an UOWC channel, which can be given as a double Gamma function to describe the channel [34]. According to simulations reported, the effect of multiple photon scattering led to an impulse spread up to 3 ns for 40 m of coastal water ($k = 0.398$ m^{-1}) and around 6 ns for 12 m of turbid water ($k = 2.19$ m^{-1}). For these values, the 3-dB bandwidth of the channel is always higher than 100 MHz, leading to a negligible the Inter-Symbol Interference (ISI) in our case. A simplified expression for the received signal power can be thus derived to express the variation of the received power vs. the distance d, on axis:

$$P_{opt}(d) = \frac{P_1}{d^2} \exp(-k(\lambda)d) \qquad (3)$$

where P_1 is the power received at 1 m ($P_1 \cong 1.2$ mW, measured in lab). Typical values of absorption and scattering coefficients are reported in Table I [13], [19].

TABLE I

TYPICAL VALUES OF ABSORPTION AND SCATTERING COEFFICIENTS [13], [19]

Water type	a (m^{-1})	b (m^{-1})	k (m^{-1})
Pure sea water	0.040	0.002	0.043
Clear ocean	0.114	0.037	0.151
Coastal ocean	0.179	0.219	0.399
Turbid coastal water	n.a.	n.a.	0.8

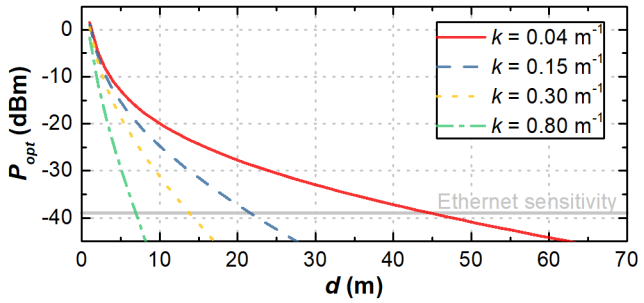

Fig. 2. Simulated received power as a function of the transmission distance at different value of water turbidity. The straight gray line indicates the receiver sensitivity for the Ethernet 10Base-T transmission obtained in dark environment (see section IV).

Clearly, a transmission in turbid coastal water is far more challenging than pure clear water.

We note that (3) is a valid approximation for $kd < 10$ (in our experiments, we always have $kd < 3$) [35]. If $kd > 10$, the received signal would have shown lower attenuation, because of the multiple scattering [35]. Furthermore, the channel can be assumed as linear since nonlinear effects (mostly Raman and Kerr) can be neglected because of the wide optical spectrum and limited power of our TX. Thus (3) can be a valid approximation in our case (we outline that we neglected turbulence effects, which are not expected to be relevant in our short-distance links). From Table I, we also estimated the received optical power at certain distances, considering different values of water turbidity. We show in Fig. 2 the curves calculated using (3) with $P_1 = 1.2$ mW and $A_{RX} = 100$ mm^2. The simulation is based on the assumption of 20° emission angle and a transmission along the optical axis ($\varphi = \psi = 0°$). We chose $k = 0.04, 0.15, 0.3, 0.8$ m^{-1}, i.e., from the clearest ocean waters to extremely murky waters. We measured the sensitivity of our RX to be -39 dBm (as will be presented in detail in section IV). This is the minimum optical power required to correctly receive the Ethernet signal in dark condition (no background noise). Given this value, we can obtain a practical estimation of the maximum achievable link distance, in different water conditions: for the above values of k, the estimated maximum transmission distance ranges from 7 to 45 m.

III. OPTICAL MODEM DESIGN

In this section, we discuss the key elements involved in the design of our UOWC modems.

A. Optical Section of the Modems

Both modems are constituted of three sections: TX, RX and the monitoring part. The three parts were assembled in three consecutive transversal sections of a cylindrical support (see Fig. 3). The electrical scheme of the optical section of one of modems and its final implementation are also shown in Fig. 3.

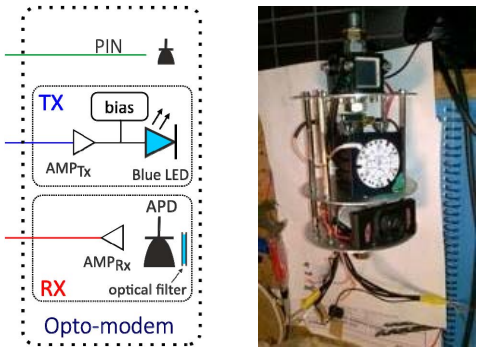

Fig. 3. Scheme of the UOWC modem (left) and the picture of one of the UOWC optical modems (right). The three floors contain (from top to bottom): the monitoring photodiode, the transmitter LEDs and the receiver.

The TX was made by a LED array of seven chips with the emission peak at 470 nm, 20 nm optical bandwidth. Blue light was chosen to obtain the minimum attenuation in clean water; although the modems are first meant to prove shallow water transmission, the main operative scenario in future will be deep clear waters. The LED chips were connected in series and biased at 21 V (around 400 mA), giving a total luminous flux of ~300 lm. The signal from the Ethernet interface (Manchester-coded signal with 10 Mbit/s data rate [36]), after an amplification stage (Amp_{TX}, 25 dB gain, 130 MHz 3-dB bandwidth), was superimposed to the dc bias voltage of the LED by means of a bias-tee. A lens was used to further shape the beam, increasing the optical density at the receiver. The Lambertian pattern of the LED beam was reduced down to 20° using a proper low-cost plastic lens. In the aligned condition, this lens led to an optical gain around 11 dB.

The RX encompasses an APD module with an integrated transimpedance amplifier (TIA). The APD had an active area of 100 mm^2 and a frequency cut-off of 11 MHz.

We conveniently placed a 30 nm bandwidth blue-filter in front of the APD and we also reduced the Field Of View (FOV) of the RX down to 70° (see details on section III.C). The output of the APD was then properly amplified by a variable voltage amplifier (10 to 40 dB gain). This amplifier (Amp_{RX}) was needed to produce a signal with the electrical amplitude compliant with Ethernet interface standards. Finally, a monitoring layer was added to the previous ones, with one cheap pin-photodiode (PIN); this solution allows to detect and measure the amount of light present at the RX.

All used devices are commercially available and have limited cost, which could make the final prototypes suitable to be massively deployed over several AUVs.

B. Water Turbidity

As explained in section II, the UOWC performance is strongly affected by scattering and absorption. In order to measure the k value in our sea location, in the first sea trials

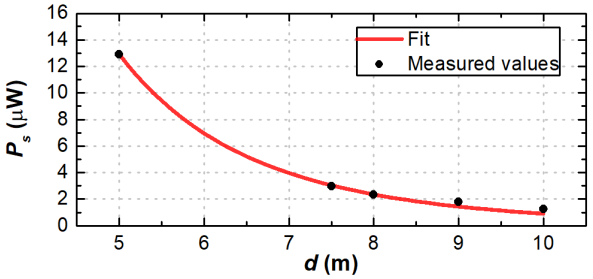

Fig. 4. Measured received optical power at different distance between the modems. The fitting curve is based on the theoretical expression of the propagation of a Lambertian pattern.

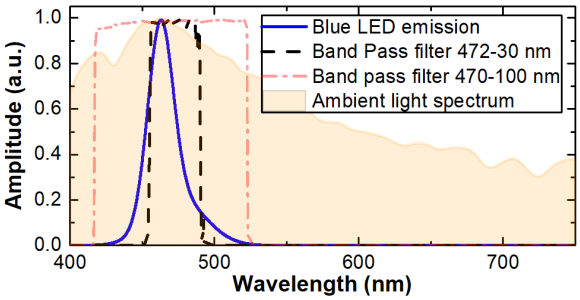

Fig. 5. Optical spectra of the ambient light, blue LED and band-pass filters under test. The sunlight spectrum has been taken at noon, during a sunny day.

we placed two modems underwater, turned on the TX and used the PIN as a monitor to measure the received optical power (P_s) at different distances. To measure P_s, we drove the LED with a periodic square-wave with 50% duty cycle and 6 seconds period, in such a way that the LED was off and on alternatively. During the TX blinking, we measured the current flowing through the PIN for 10 periods. From the corresponding average values of current during on and off times, we could measure the total power at the receiver and the noise power. By subtracting the second to the first, we could reliably estimate the true signal power P_s. We had to introduce this solution since both signal and background fluctuate. Particularly, the background is strongly affected by occasional speckles from the sunlight, which are due to the sea waves and can randomly reach the RX.

We report in Fig. 4. the measured optical values as a function of the distance d between the modems, in a single specific day for consistency (k coefficient is expected to change randomly, even in the same location). Due to time constrain for the trial, we decided to take measurements only at distances mostly useful for the communication point of view. In this figure we also show the fitting curve based on (3). The fitting gives us a $P_1 = 1.15$ mW and $k = 0.25$ m^{-1}. The P_1 value shows excellent agreement with the value taken in laboratory at 1 m free-space (1.2 mW), confirming the goodness of the fit.

During the experiment, we measured the turbidity by means of the turbidimeter, in terms of Formazin Turbidity Unit (FTU). The value was found in the range between 1 and 1.5 FTU, from which we can obtain another estimation of the k coefficient; it was previously reported that k and FTU values are related by a linear relationship with a slope coefficient of k/FTU ≈ 0.2 [37]. According to this approach, our FTU corresponds to a k value between 0.2 and 0.3 m^{-1}, which confirms the fitting results.

We also note that experimental evidence was reported about a relationship between the light penetration in water and its turbidity, indicating that typical harbor water has $k \sim 0.3$ m^{-1} [38]. These values are all related to a single measurement event. It must be stressed that, even in the same location and after few hours, we can realistically expect quite worse (or better) k values.

C. Background Noise

In practical cases (especially in shallow waters), the background light (sunlight) can have high values: in the first tests, we measured more than 10^4 lux on the pier, due to sunlight. This is a relevant value, which, even assuming the effect of the filter at the RX, produces a photo-current comparable with signal current: therefore it is expected that the background noise can limit the performance of UOWC links.

The background noise obviously depends on the working depth: e.g. deep ocean is by far less noisy then shallow harbor waters. However, in order to have modems capable of working in all conditions, the impairments due to sunlight in UOWC cannot be simply neglected and they must be carefully taken into account when designing the optical system. The ambient light received by the photo-detector P_{bkg} can be factorized with several parameters, given by this expression:

$$P_{bkg} = A_{Rx}(\pi FOV)^2 f(\Delta\lambda) L_{SUN}(\Delta\lambda) \tag{4}$$

where A_{RX} is the active area of the receiver, FOV is the Field-of-View of the RX, $f(\lambda)$ and $\Delta\lambda$ are the optical band-pass transmittivity and the bandwidth of the RX filter, and L_{SUN} the solar radiance at the same wavelength window.

In order to minimize the effect of background light, we acted on some of these parameters in the design of the optical modem: active area, FOV and characteristics of the filter in front of the APD. Then, we conveniently used a blue filter to reject most of the ambient light. Whilst the center wavelength of the filter was an obvious choice to match the LED peak wavelength, the bandwidth of the filter has been chosen to maximize the signal to background power ratio.

We tested two different blue filters. The first filter has a bandwidth of 100 nm, which covers all the emission spectrum of the TX, while the second filter has a bandwidth of 30 nm, comparable with the LED emission (20 nm), hence the tails of the emission were cut by the filter (see Fig. 5). The background spectrum was taken by means of a photometer (0.5 nm resolution), placed just above the water surface pointing horizontally. The spectrum was taken at sea-trials around noon, during a sunny day in July. Considering normalized amplitudes, the gain in OSNR with the narrower filter is around 3 dB. Although the 30 nm filter slightly reduced the optical power from the LED by 1 dB, it rejected a greater portion of the background light.

Another feature of the background sunlight is its directionality: sunlight can arrive at the RX directly or because of Rayleigh scattering both in the atmosphere and in water. Our source is positioned horizontally, in front of the receiver.

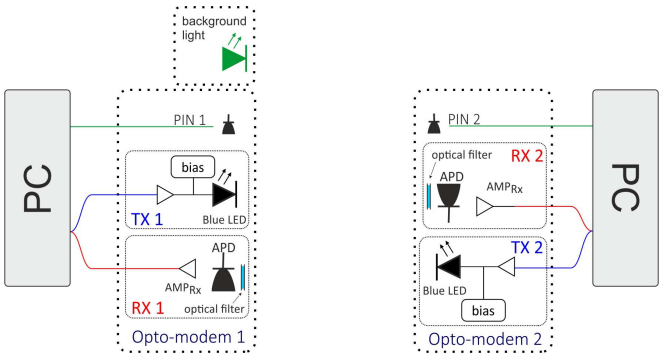

Fig. 6. Scheme of experimental setup to test resilience to background light; a pair of optical modems are placed one in front of each other (DLOS configuration). On one side, an auxiliary optical source is used to simulate the background light.

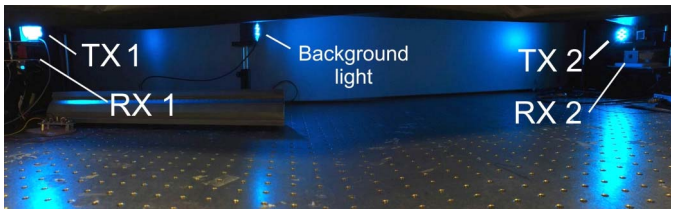

Fig. 7. Picture of the lab experimental setup.

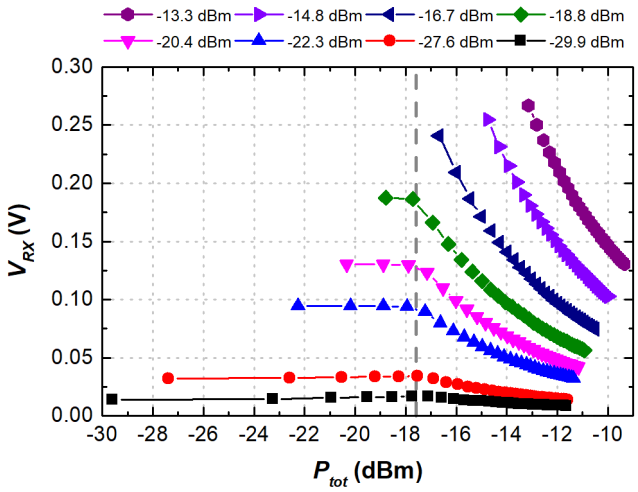

Fig. 8. V_{RX} as a function of the received optical power P_{tot} (signal plus background light). The curves are taken at different P_s indicated on top. The vertical dashed line indicates the threshold, above which V_{RX} reduces.

At different hours, seasons and weather conditions, the sunlight can be directional, rather than diffused, and can be closer or farther to the transmission axis.

It can then be seen that reducing the FOV of the RX in our condition preserves the signal optical power at the receiver but can strongly limit the impact of the incident background noise. This is of course not a general statement: if the modem is operated in a dark environment, a wider FOV can allow to collect some more signals and could be beneficial. In our case, we shrunk the FOV by a mechanical frame mounted in front of the APD. Common FOV for a planar receiver is around 180° (2θ angle); it is reduced down to 70° using the frame.

We also measured that the entire sunlight spectrum corresponds to around 4.5 dBm at noon. From this value, we estimated a received background optical power (P_{bkg}) of about -6 dBm, considering the active area of the photo-detector, the effect of the optical filter, the water attenuation, and the FOV reduction of the photo-detector.

IV. Laboratory Tests

Before the sea-trials experiments, we performed a wide number tests in the lab, spanning various issues of the UOWC system. As mentioned before, one of the main source of noise for the system is the ambient light; hence, we characterized the behavior of the APD under strong background light.

A. Experimental Set-Up

For this analysis, we realized the experimental setup shown in Fig. 6 and with a picture in Fig. 7.

TX and RX were placed in directed line-of-sight (DLOS) configuration and covered with a black screen, blocking light from uncontrolled external optical sources. A controlled background noise was then emulated by a secondary un-modulated blue LED source (with the same wavelength used for the TX). Thus, all the produced noise was in the transmittance band of the optical filter. The optical power of the signal was controlled by optical attenuators placed in front of the TX. With this setup, we were able to simulate various environmental conditions, such as different transmission distances and different levels of ambient light, performing transmission measurements with different OSNR.

To test the system, we connected the modems to the Ethernet interfaces of two PCs. We then used a software to generate and send random data packets; it then also allows measuring the packet loss at the RX. We stress that, given the design constrains due to the final Ethernet implementation, common bit error rate measurements cannot be carried out in this case, thus only packet loss values can be reported. For this test bench, all the devices were powered by lab power supplies. The received optical powers (both signal and noise) were measured with a PIN placed next to the APD and rescaled to take into account the different active areas and responsivity.

B. APD Saturation

We first characterized the impact of the CW light on the RX performance due to saturation, which is induced by both signal and background light on the receiver module (APD and TIA). To this aim, we set a given value of the TX optical power (P_S) and modulated the TX LED with a 1 MHz sinewave. Then, we measured the amplitude of the RX output signal (V_{RX}), as a function of the intensity of the ambient light P_{bkg} (by changing the bias current of the unmodulated LED). The measurements were repeated at different P_S values. The experimental results are shown in Fig. 8. Here, we report the V_{RX} values as a function of the total received power ($P_{tot} = P_s + P_{bkg}$). The values of P_{tot} naturally started from around P_s(i.e., P_{bkg} negligible) for each curve.

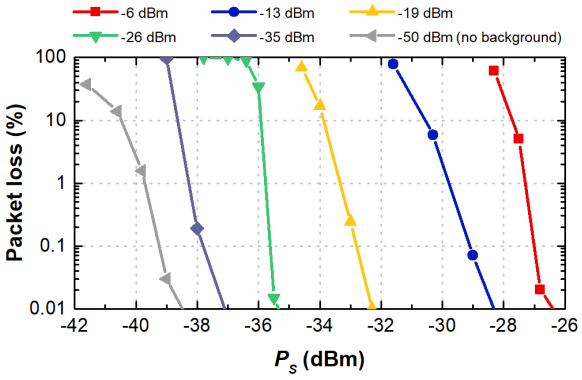

Fig. 9. Packet loss measurements as a function of the signal power P_s. The measurements were taken with different P_{bkg} values reported on top.

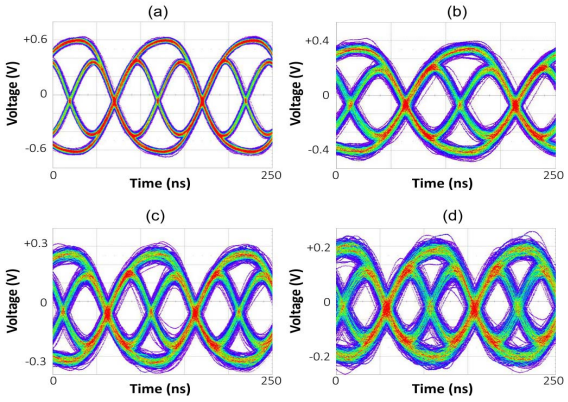

Fig. 10. Eye Diagrams taken with $P_{bkg} = -19$ dBm and at different P_s: -28 dBm (a); -32 dBm (b); -33 dBm (c); -34.5 dBm (d).

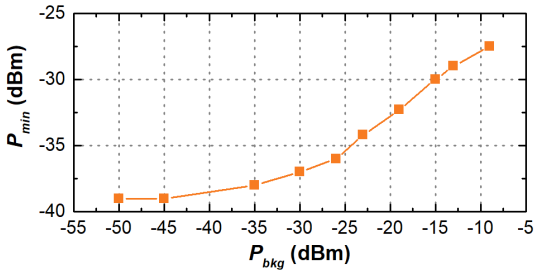

Fig. 11. Signal optical power required to guarantee a transmission in error-free condition for specific value of background light.

As expected V_{RX} is higher with higher P_s, while, increasing P_{bkg}, V_{RX} remains constant until the total received power reaches -17.5 dBm (highlighted in the figure with the vertical dashed gray line). Above this value, any further increase of the P_{bkg} reduces the signal amplitude at the RX output. We highlight that this will be the most common working condition, because the received ambient light in normal condition is around -6 dBm, i.e. it is much higher than this saturation value.

C. System Performance

From the previous results, we have to expect a significant increase of RX sensitivity in the usual operating conditions, from the values observed in the dark. It was thus needed to characterize the UOWC system before the sea field tests, by measuring the impact of the background on the system performance. We sent 600'000 Ethernet packets to the TX and measured the packet loss at the RX output as function of the received signal power. We present these results in Fig. 9. Here the different curves were obtained for different values of background light (represented in different colors). The considered background intensities range from dark condition (-50 dBm), to our typical average sunlight (-6 dBm).

As can be seen, we have a step-like behavior in the packet loss measurements. This is mainly due to the signal threshold of the Ethernet interface, even if the quality of the signal was still good.

As example of signal degradation, we report in Fig. 10 various eye diagrams taken varying P_s from -28 to -34.5 dBm, at a fixed background light ($P_{bkg} = -19$ dBm). We outline that these eye diagrams are typical of the Manchester-coded signal (IEEE 802.3), where at the center of the bit there is always a transition (i.e., in our AC-coupled case, the waveform crossed the zero axis). These eye diagrams represent four significant cases. The first eye diagrams was taken with the system in an optimal condition ($P_s = -28$ dBm, no packet loss); the second eye diagram was taken at lower power ($P_s = -32$ dBm), and still error-free; the third one, taken at just 1 dB lower power ($P_s = -33$ dBm) was observed with some non-negligible packet loss (<1%). Finally the last eye was taken at $P_s = -34.5$ dBm, when the packet loss was greater than 60%. In all cases, we observe clearly a threshold-like behavior, where for any P_{bkg} value we can find a minimum required power P_{min} to correctly operate the system.

From the data showed in Fig. 9, we extrapolated the P_{min} values for any specific value of ambient light P_{bkg}. This curve is reported in Fig. 11. As can be seen, there is no linear relation between the P_{min} and P_{bkg}, keeping in mind also the saturation effect on the APD at high optical power. These data give a quantitative means to predict the behavior of the system under moderate and strong illumination condition.

As example, after this characterization of the optical modems, we expect that our UOWC system can work even with strong ambient light of 4.5 dBm/cm^2 (sunny day in summer) when received signal power P_s is at least -26 dBm.

Depending on the water turbidity, different transmission distances can be achieved. For example, considering a $k = 0.25$ m^{-1}, a distance of 8 m can be achieved (see Fig. 2). Considering a dark environment, an estimated distance of 13 m can be achieved with same condition of water turbidity.

V. Watertight Container

The modems pressure hull has been designed and realized as composed by an assembly of two parts: the body (containing power and Ethernet signal boards) and the head (containing the optical layer as described above). Both parts are composed by a cylindrical tube, enclosed between two acetal neck flanges. While the body tube is made from a 6xxx-series anticorodal aluminum alloy, the head case is made from Perspex. Both tubes have been bonded to the corresponding flange necks

Fig. 12. Strength and leakage tests at CMRE, La Spezia.

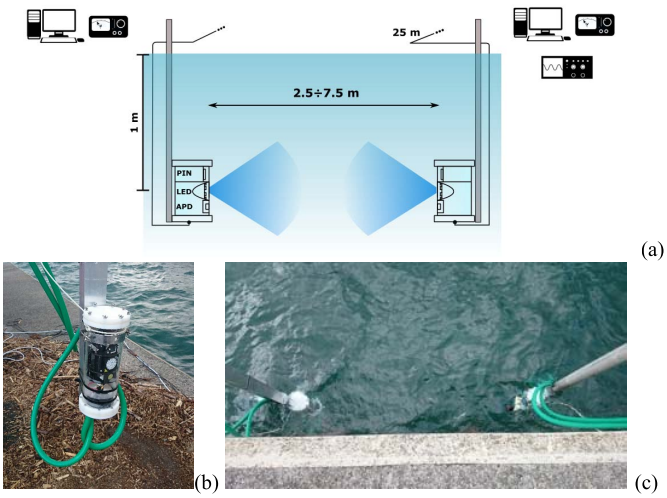

Fig. 13. Experimental setup of the sea trials measurements (a) and picture (c); poles and connection cables can be clearly seen. (b) Watertight container of one modem, with umbilical cords (green).

using a special sealing adhesive, commonly used in marine applications. For the sea trials of the present paper only the head case shown on Fig. 12 has been used.

The upper flange of the head is closed by an acetal blind flange constrained by six bolted screws. In order to prevent any water leakage, a double radial o-ring seal was realized between the blind flanges and the corresponding internal surfaces of the necks. The o-ring glands have been designed and manufactured according to the guidelines provided by common seal manuals and handbook. In order to verify the possibility to employ the pressure hulls during a mission, the parts have been tested in a custom pressure chamber available at the CMRE facility, La Spezia. The head, being a 3-mm wall tube and made from Perspex, was tested to reach 50 m depth maintaining its full integrity and the required watertight properties. Failure depth for the head pressure hull was measured at about 60 m depth.

VI. Sea Trial

As final demonstration, we performed various sea-trials to test the system performance in a real sea environment. The trials were conducted at the harbor of La Spezia (Italy). The experimental area is located in the middle of two piers and only open to research activities. We could access a pier, where the modems could be submerged and, at the same time, we could keep both connected by cables (see Fig. 13b):

TABLE II
Experimental Data Recorded at Different Distances

d (m)	P_{bkg} (dBm)	Est. P_s (dBm)	Turbidity (FTU)	Packet Loss (%)
2.5	-5.5	-10.1	1-1.5	0
5.0	-5	-18.9	1-1.5	0
7.5	-6.7	-25.2	1-1.5	0.04

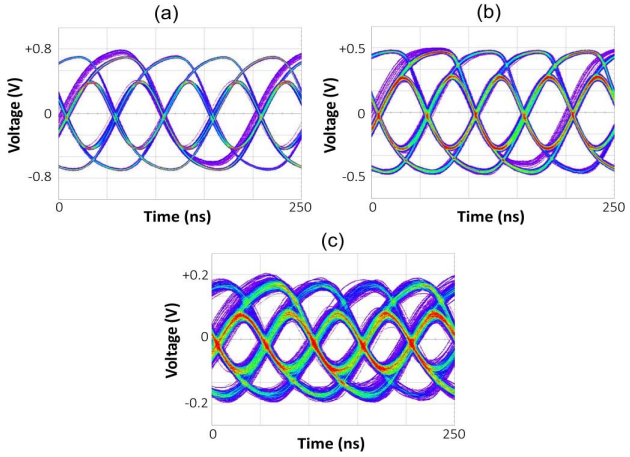

Fig. 14. Eye diagrams recorded at 2.5 (a), 5.0 (b) and 7.5 m (c).

the connection allowed us to control the modems, to send/receive data and to measure the transmission performance using the monitoring equipment in a container on the pier. Here, the water turbidity is much higher than in an open sea.

In this first sea-trial, we experimentally tested a version of the modems where only the optical layer was underwater. The setup for the sea experiments is sketched in Fig. 13, where we also report the picture of the submerged modems. The modems were clamped to two poles; one was fixed to the pier and the other movable (along the pier) by means of a forklift. Both modems were submerged so that the optical layers were around 1 m depth. All the other equipment (power supplies, PCs, real-time oscilloscope, etc…) was inside a container nearby on the pier, connected with 25 m long coaxial cables. The tests consisted in packet loss measurements as a function of the distance (starting from 2.5 m). During these measurements, the environmental conditions were also acquired. Using the monitor photodiode, we measured the P_{bkg} at different distances and with the turbidimeter we recorded the water turbidity in terms of FTU. These values can change during the packet loss measurements. A summary of these measurements is presented in Table II, where P_{bkg}, P_s, turbidity and packet loss values are shown.

After each transmission test, we also acquired the eye diagrams of the received waveforms with a real-time oscilloscope. These diagrams are reported in Fig. 14, at 2.5 m (a), 5.0 m (b), 7.5 m (c) distances. From this figure, we can clearly see that evolution of the eye opening with longer distances. However, despite the wide open eyes, in the last case (c), we recorded a non-zero packet loss (0.04 %) after a transmission of 14457 packets.

VII. Conclusion

Using common LEDs as transmitter, we designed and demonstrated a novel UOWC system, useful for practical marine experiments and fully compatible with 10Base-T Ethernet transmission (10 Mbit/s with a Manchester-coded signal). The modem includes a photonic section, an electronic part and are enclosed in a water-proof hull.

We first tested the system in controlled environments (lab and pressure chamber). Then the system was also tested in a real sea environment, with modems submerged by 1 m, in murky harbor waters, under strong sunlight. In order to reach stable and successful operation, we had to minimize the effects of the background light (sunlight): to this aim, we performed a deep analysis of the UOWC system under various environmental conditions to properly design the optical layer of the modem. This analysis has led to a successful implementation, which allowed us achieving up to 5 m in error-free condition and up to 7.5 m with a minimum packet loss. These results represent an encouraging step to reach the target of the OptoCOMM/SUNRISE project, where a transmission distance of 10 m and a complete integration of the software is expected to be reached. A report of the final sea-trials measurements will be presented with more details in future with the description of the comprehensive work done integrating the present optical layer with the electro-mechanical and firmware parts. This will prove the effective integration of our modems in a node of the Littoral Ocean Observatory Network (LOON) test-bed of the SUNRISE infrastructure.

Finally, we outline that the sea-trial conditions were chosen to be very stressing, with strong turbidity and high sunlight. It is known that in typical open-sea waters, the turbidity is much lower: in that case, at same sunlight illumination conditions, the transmission distance can be effectively extended with a reach exceeding 15 m. This value would further increase at greater depth values, where sunlight would be absorbed by the water. In that case, a reach exceeding 40 m is expected. Future developments can provide higher distances, mobility, reliability and the miniaturization of the modems.

VIII. Acknowledgments

The authors gratefully acknowledge the personnel of the Centre for Maritime Research and Experimentation (CMRE) and of the Naval Support and Experimentation Centre of Italian Navy (CSSN), particularly the technical support from P. Guerrini and J. Alves. The authors also acknowledge stimulating discussions with A. Caiti, R. Nuti and S. Grechi.

References

[1] K. Alam, T. Raym, and S. G. Anavatti, "A brief taxonomy of autonomous underwater vehicle design literature," *Ocean Eng.*, vol. 88, pp. 627–630, Sep. 2014.

[2] S.-K. Jeong *et al.*, "Design and control of high speed unmanned underwater glider," *Int. J. Precis. Eng. Manuf.-Green Technol.*, vol. 3, no. 3, pp. 273–279, Jul. 2016.

[3] T. Battista, C. Woolsey, T. Perez, and F. Valentinis, "A dynamic model for underwater vehicle maneuvering near a free surface," *IFAC-PapersOnLine*, vol. 49, no. 23, pp. 68–73, 2016.

[4] M. Kojima *et al.*, "AUV IRSAS for submarine hydrothermal deposits exploration," in *Proc. IEEE/OES Auto. Underwater Vehicles (AUV)*, Nov. 2016, pp. 161–164.

[5] S. D. Ling, I. Mahon, M. P. Marzloff, O. Pizarro, C. R. Johnson, and S. B. Williams, "Stereo-imaging AUV detects trends in sea urchin abundance on deep overgrazed reefs," *Limnol. Oceanogr., Methods*, vol. 14, no. 5, pp. 293–304, May 2016.

[6] S. Sendra, J. V. Lamparero, J. Lloret, and M. Ardid, "Study of the optimum frequency at 2.4 GHz ISM band for underwater wireless ad hoc communications," in *Proc. Int. Conf. Ad-Hoc Netw. Wireless*, 2012, pp. 260–273.

[7] S. I. Inácio, "Dipole antenna for underwater radio communications," in *Proc. IEEE 3rd Underwater Commun. Netw. Conf. (UComms)*, Aug./Sep. 2016, pp. 1–5.

[8] E. Jimenez *et al.*, "Investigation on radio wave propagation in shallow seawater: Simulations and measurements," in *Proc. IEEE 3rd Underwater Commun. Netw. Conf. (UComms)*, Aug./Sep. 2016, pp. 1–5.

[9] U. M. Qureshi *et al.*, "RF path and absorption loss estimation for underwater wireless sensor networks in different water environments," *Sensors*, vol. 16, no. 6, p. 890, 2016.

[10] J.-H. Cui, J. Kong, M. Gerla, and S. Zhou, "The challenges of building mobile underwater wireless networks for aquatic applications," *IEEE Netw.*, vol. 20, no. 3, pp. 12–18, May/Jun. 2006.

[11] D. E. Chaitanya, C. V. Sridevi, and G. S. B. Rao, "Path loss analysis of underwater communication systems," in *Proc. IEEE Technol. Symp. (TechSym)*, Jan. 2011, pp. 65–70.

[12] B. Li *et al.*, "Further results on high-rate MIMO-OFDM underwater acoustic communications," in *Proc. OCEANS*, Sep. 2008, pp. 1–6.

[13] H. Kaushal and G. Kaddoum, "Underwater optical wireless communication," *IEEE Access*, vol. 4, pp. 1518–1547, 2016.

[14] S. Arnon, "Underwater optical wireless communication network," *Opt. Eng.*, vol. 49, no. 1, pp. 015001–015006, 2010.

[15] G. Cossu, R. Corsini, and E. Ciaramella, "High-speed bi-directional optical wireless system in non-directed line-of-sight configuration," *J. Lightw. Technol.*, vol. 32, no. 10, pp. 2035–2040, May 15, 2014.

[16] G. Cossu, A. Wajahat, R. Corsini, and E. Ciaramella, "5.6 Gbit/s downlink and 1.5 Gbit/s uplink optical wireless transmission at indoor distances ($\geq$ 1.5 m)," in *Proc. Eur. Conf. Opt. Commun. (ECOC)*, Sep. 2014, pp. 1–3.

[17] V. Jungnickel *et al.*, "A European view on the next generation optical wireless communication standard," in *Proc. IEEE Conf. Standards Commun. Netw. (CSCN)*, Oct. 2015, pp. 106–111.

[18] M. Uysal, C. Capsoni, Z. Ghassemlooy, A. Boucouvalas, and E. Udvary, Eds. *Optical Wireless Communications: An Emerging Technology*. Cham, Switzerland: Springer, 2016. [Online]. Available: http://www.springer.com/gp/book/9783319302003

[19] J. W. Giles and I. N. Bankman, "Underwater optical communications systems. Part 2: Basic design considerations," in *Proc. IEEE Military Commun. Conf. (MILCOM)* Oct. 2005, pp. 1700–1705.

[20] A. C. Boucouvalas, K. P. Peppas, K. Yiannopoulos, and Z. Ghassemlooy, "Underwater optical wireless communications with optical amplification and spatial diversity," *IEEE Photon. Technol. Lett.*, vol. 28, no. 22, pp. 2613–2616, Nov. 15, 2016.

[21] B. M. Cochenour, L. J. Mullen, and A. E. Laux, "Characterization of the beam-spread function for underwater wireless optical communications links," *IEEE J. Ocean. Eng.*, vol. 33, no. 4, pp. 513–521, Oct. 2008.

[22] H. Zhang and Y. Dong, "Impulse response modeling for general underwater wireless optical MIMO links," *IEEE Commun. Mag.*, vol. 54, no. 2, pp. 56–61, Feb. 2016.

[23] K. Nakamura, I. Mizukoshi, and M. Hanawa, "Optical wireless transmission of 405 nm, 1.45 Gbit/s optical IM/DD-OFDM signals through a 4.8 m underwater channel," *Opt. Exp.*, vol. 23, no. 2, pp. 1558–1566, 2015.

[24] H. M. Oubei *et al.*, "4.8 Gbit/s 16-QAM-OFDM transmission based on compact 450-nm laser for underwater wireless optical communication," *Opt. Exp.*, vol. 23, no. 18, pp. 23302–23309, 2015.

[25] J. Xu *et al.*, "OFDM-based broadband underwater wireless optical communication system using a compact blue LED," *Opt. Commun.*, vol. 369, pp. 100–105, Jun. 2016.

[26] G. Cossu, A. M. Khalid, R. Corsini, and E. Ciaramella, "Non-directed line-of-sight visible light system providing high-speed and robustness to ambient light," in *Proc. Opt. Fiber Commun. Conf. Expo. Nat. Fiber Opt. Eng. Conf. (OFC/NFOEC)*, Mar. 2013, pp. 1–3.

[27] *SUNRISE: Building the Internet of Underwater Things*. Accessed: Jan. 2017. [Online]. Available: http://fp7-sunrise.eu/

[28] A. Bartolini *et al.*, "OptoCOMM: Development and experimentation of a new optical wireless underwater modem," in *Proc. MTS/IEEE Monterey OCEANS*, Sep. 2016, pp. 1–5.

[29] A. Caiti *et al.*, "OptoCOMM: Introducing a new optical underwater wireless communication modem," in *Proc. IEEE 3rd Underwater Commun. Netw. Conf. (UComms)*, Aug./Sep. 2016, pp. 1–5.
[30] D. J. Segelstein, "The complex refractive index of water," Ph.D. dissertation, Dept. Phys., Univ. Missouri–Kansas City, Kansas City, MO, USA, 1981.
[31] N. G. Jerlov, *Marine Optics*. Amsterdam, The Netherlands: Elsevier, 1976.
[32] E. F. Schubert, T. Gessmann, and J. K. Kim, *Light Emitting Diodes*. Hoboken, NJ, USA: Wiley, 2005.
[33] Y. Ito, S. Haruyama, and M. Nakagawa, "Short-range underwater wireless communication using visible light LEDs," *WSEAS Trans. Commun.*, vol. 9, pp. 525–552, 2010.
[34] S. Tang, Y. Dong, and X. Zhang, "Impulse response modeling for underwater wireless optical communication links," *IEEE Trans. Commun.*, vol. 62, no. 1, pp. 226–234, Jan. 2014.
[35] B. Cochenour, L. Mullen, and J. Muth, "Effect of scattering albedo on attenuation and polarization of light underwater," *Opt. Lett.*, vol. 35, no. 12, pp. 2088–2090, 2010.
[36] *IEEE Standard for Local and Metropolitan Area Networks—System Considerations for Multisegment 10 Mb/S Baseband Networks (Section 13) and Twisted-Pair Medium Attachment Unit (MAU) and Baseband Medium, Type 10BASE-T (Section 14)*, IEEE Standard 802.3i-1990, 1990.
[37] U. Lumborg and K. Bundgaard, "Studies of the relationship between suspended sediment concentration and light attenuation," in *Proc. 13th Int. Conf. Cohesive Sediment Trans. Process. (INTERCOH)*, Leuven, Belgium, Sep. 2015, pp. 64–65.
[38] W. A. Swenson, *Influence of Turbidity on Fish Abundance in Western Lake Superior*, document EPA-600/3-78-067, Environmental Protection Agency, Office of Research and Development, Environmental Research Laboratory, 1978.

Giulio Cossu received the M.S. degree in physics from the University of Pisa in 2010 and the Ph.D. degree from the Scuola Superiore Sant'Anna in 2014. Since 2014, he has been a Research Fellow with the Scuola Superiore Sant'Anna. He participated at several Italian and European research projects (ROAD–NGN, INFIERI, SUNRISE, and OPTICWISE). He has published over 40 international papers. He has co-authored one international patent. His research interests include the areas of passive optical network and orthogonal frequency division multiplexing modulation, and the investigation of innovative solutions of optical wireless communications.

Alessandro Sturniolo received the master's degree in materials science from Tor Vergata University, Rome. He is currently pursuing the Ph.D. degree in photonic technologies with the Scuola Superiore Sant'Anna. He is currently working on VLC-based indoor positioning. The main topics in his research are visible light communications (VLCs) and optical wireless systems for indoor as well as for harsh environment.

Alessandro Messa received the master's degree in biomedical engineering from the La Sapienza University of Rome. He has done his thesis at The Institute of Cancer Research of London about "Optical Coherence Tomography for Shear Wave Elastography." His research activity continued as responsible for the project "Ultrasound 3D Tomography for the Evaluation of Breast Cancer Risk" until 2015. Back in Italy, he was an IT Validation Consultant in the pharmaceutical sector and then as a Java Developer in the IT consulting sector. The main topics in his research are visible light communications and optical wireless.

David Scaradozzi received the B.Eng., M.Eng. in automation engineering, Ph.D. degrees. He is currently an Accredited Engineer and an Assistant Professor with the Dipartimento di Ingegneria dell'Informazione and a Mobility Delegate of the Engineering Faculty with UNIVPM, Chercheur Associé, LSIS, UMR CNRS 6168, Marseille, France. He has expertise in the field of marine robotics and artificial intelligent systems. He is a member of the Ph.D. School in Information Engineering, where he is the Chair of the course "Advanced virtual instruments for simulation and control of complex systems." He is the Chair of the course "Control Systems Design and Optimization." His research activities are in the field of control and optimization of dynamical systems, robotics, and automation and educational robotics.

Ernesto Ciaramella received the Laurea degree in physics from the La Sapienza University, Rome, in 1991. He is currently a Professor of communications with Scuola Superiore S. Anna, Pisa. In 1992, he was awarded a scholarship by Alcatel on optical coherent communication systems. From 1992 to 1994, he was a Contract Researcher with Fondazione Ugo Bordoni, where he was involved in nonlinear optical effects. From 1994 to1998, he was with CSELT, Turin, concerned with design and realization of optical systems. From 1998 to 2000, he was a Scientific Researcher at Fondazione Ugo Bordoni, where he was involved in optical systems and network. From 2001 to 2002, he was a Research Manager with CNIT National Photonic Networks Laboratory, Pisa. Since 2002, he has been with the Scuola Superiore Sant'Anna, where he started and is leading a research group on optical transmission systems. He published around 200 international papers. He has co-authored 22 international patents. His main research interests include the design of WDM systems for transport and access networks, optical processing, and free-space optical systems (optical wireless). He participated in several European research projects (OPEN, PHOTOS, ATLAS, NOBEL, SUNRISE, and INFIERI). He has been a Coordinator of the FP7 project COCONUT from 2012 to 2016. He has been serving as a reviewer for various international journals and in technical program committees of several optical communication conferences. Since 2012, he has been serving as an Associate Editor of the IEEE PHOTONICS TECHNOLOGY LETTERS.